OPEN

Citation: Cell Death and Disease (2013) 4, e742; doi:10.1038/cddis.2013.267

www.nature.com/cddis

Anticancer compound ABT-263 accelerates apoptosis in virus-infected cells and imbalances cytokine production and lowers survival rates of infected mice

L Kakkola[1,11], OV Denisova[1,11], J Tynell[2], J Viiliäinen[3], T Ysenbaert[4], RC Matos[1], A Nagaraj[1], T Öhman[3], S Kuivanen[5], H Paavilainen[6], L Feng[7], B Yadav[1], I Julkunen[2], O Vapalahti[5,8], V Hukkanen[6], J Stenman[1,7], T Aittokallio[1], EW Verschuren[1], PM Ojala[3,9], T Nyman[3], X Saelens[4], K Dzeyk[10] and DE Kainov*[,1]

ABT-263 and its structural analogues ABT-199 and ABT-737 inhibit B-cell lymphoma 2 (Bcl-2), BCL2L1 long isoform (Bcl-xL) and BCL2L2 (Bcl-w) proteins and promote cancer cell death. Here, we show that at non-cytotoxic concentrations, these small molecules accelerate the deaths of non-cancerous cells infected with influenza A virus (IAV) or other viruses. In particular, we demonstrate that ABT-263 altered Bcl-xL interactions with Bcl-2 antagonist of cell death (Bad), Bcl-2-associated X protein (Bax), uveal autoantigen with coiled-coil domains and ankyrin repeats protein (UACA). ABT-263 thereby activated the caspase-9-mediated mitochondria-initiated apoptosis pathway, which, together with the IAV-initiated caspase-8-mediated apoptosis pathway, triggered the deaths of IAV-infected cells. Our results also indicate that Bcl-xL, Bcl-2 and Bcl-w interact with pattern recognition receptors (PRRs) that sense virus constituents to regulate cellular apoptosis. Importantly, premature killing of IAV-infected cells by ABT-263 attenuated the production of key pro-inflammatory and antiviral cytokines. The imbalance in cytokine production was also observed in ABT-263-treated IAV-infected mice, which resulted in an inability of the immune system to clear the virus and eventually lowered the survival rates of infected animals. Thus, the results suggest that the chemical inhibition of Bcl-xL, Bcl-2 and Bcl-w could potentially be hazardous for cancer patients with viral infections.
Cell Death and Disease (2013) **4,** e742; doi:10.1038/cddis.2013.267; published online 25 July 2013
Subject Category: Immunity

ABT-263 and its structural analogues ABT-737 and ABT-199 are small molecules that have significant efficacy against human lymphoid malignancies and small-cell lung carcinoma, especially ABT-199, because it does not induce thrombocytopenia.[1,2] These three compounds bind with different affinities to B-cell lymphoma 2 (Bcl-2), BCL2L1 long isoform (Bcl-xL) and BCL2L2 (Bcl-w) proteins and displace Bak, Bad and Bax.[3] Bax, Bak and Bad mediate the release of apoptogenic molecules, including cytochrome *c,* from the mitochondria. Cytosolic cytochrome *c* complexes with apoptotic protease-activating factor 1 (APAF1), uveal autoantigen with coiled-coil domains and ankyrin repeats (UACA) and pro-caspase-9 to form the apoptosome. Caspase-9 becomes activated in this complex, empowering it to proteolytically activate 3 and 7, which cleave numerous proteins, including the downstream executioner pro-caspase-6, which, in turn,

[1]The Institute for Molecular Medicine Finland, FIMM, Helsinki 00290, Finland; [2]The National Institute for Health and Welfare, Helsinki 00271, Finland; [3]The Institute of Biotechnology, University of Helsinki, Helsinki 00014, Finland; [4]The Department for Molecular Biomedical Research, VIB and Department of Biomedical Molecular Biology, Ghent University, Ghent 9000 Belgium; [5]The Haartman Institute, University of Helsinki, Helsinki 00014, Finland; [6]The Department of Virology, University of Turku, Turku 20520, Finland; [7]The Minerva Foundation Institute for Medical Research, Helsinki 00290, Finland; [8]The Helsinki University Hospital Laboratory, Helsinki 00290, Finland; [9]The Foundation for the Finnish Cancer Institute, Helsinki 00290, Finland and [10]Proteomics Core Facility, EMBL, Heidelberg 69117, Germany
*Corresponding author: DE Kainov, The Institute for Molecular Medicine Finland, FIMM, Tukholmankatu 8, 00290 Helsinki, Finland. Tel: +3585 0415 5460; Fax: +3589 1912 5737; E-mail: denis.kainov@helsinki.fi
[11]These authors contributed equally to this work.
Keywords: innate immunity; apoptosis; Bcl-xL; infection; cytokines; virus
Abbreviations: IAV, influenza A virus; Bcl-2, B-cell lymphoma 2; Bcl-xL, BCL2L1 long isoform; Bcl-w, BCL2L2; Bad, Bcl-2 antagonist of cell death; Bax, Bcl-2-associated X protein; Mcl-1, myeloid cell leukaemia-1; BCL2L3, Bak, Bcl-2 antagonist killer 1; UACA, uveal autoantigen with coiled-coil domains and ankyrin repeats; FADD, FAS-associating death domain-containing protein; v-ATPase, vacuolar ATPase; RNR, ribonucleotide reductase; Bid, BH3-interacting domain death agonist; VDAC, voltage-dependent anion-selective channel protein 1; Bim, Bcl-2-interacting mediator of cell death; DMN1L, dynamin-1-like protein; Becn1, beclin-1; PGAM5, phosphoglycerate mutase 1; PUMA, p53 upregulated modulator of apoptosis; p53, cellular tumour antigen p53; IKZF3, ikaros family zinc finger protein 3; HEBP2, heme-binding protein 2; APAF1, apoptotic protease-activating factor 1; BBC3, Bcl-2-binding component 3; BNIPL, Bcl-2/adenovirus E1B 19 kDa-interacting protein 2-like protein; MRPL41, 39S ribosomal protein L41, mitochondrial; TP53BP2, apoptosis-stimulating of p53 protein 2; FKBP8, peptidyl-prolyl cis-trans isomerase FKBP8; BAG1, BAG family molecular chaperone regulator 1; RAF1, RAF proto-oncogene serine/threonine-protein kinase; EGLN3, Egl nine homologue 3; G0S2, G0/G1 switch protein 2; PAWR, PRKC apoptosis WT1 regulator protein; NUAK1, NUAK family SNF1-like kinase 1; DAPK1, death-associated protein kinase 1; FLII, protein flightless-1 homologue; LRRFIP2, leucine-rich repeat flightless-interacting protein 2; TOLLIP, Toll-interacting protein; TRIM21, E3 ubiquitin-protein ligase TRIM21; H2B, histone H2B; DHX9, ATP-dependent RNA helicase A; HA, hemagglutinin; M1, matrix protein 1; NS1, non-structural protein NS1; NP, nucleoprotein; RANTES, C–C motif chemokine 5, CCL5; IL-6, interleukin-6; IL-8, interleukin-8, CXCL8; IP-10, C-X-C motif chemokine 10, CXCL10; CCL2, C–C motif chemokine 2; IFN-β, interferon beta; IFN-λ, interferon lambda; TNF-α, tumour necrosis factor; IL1ra, interleukin-1 receptor antagonist protein, IL-1F3; RIG-I, retinoic acid inducible gene-I; MDA-5, melanoma differentiation-associated protein 5; TLR4, Toll-like receptor 4
Received 26.2.13; revised 23.5.13; accepted 21.6.13; Edited by G Ciliberto

activates caspase-8.[4,5] Active caspase-8 cleaves BH3-interacting domain death agonist (Bid).[6] Cleaved Bid facilitates the mitochondrial apoptosis pathway and accelerates cancer cell death.[7]

Replication of several important human microbes, such as the influenza A virus (IAV), hepatitis B virus, hepatitis C virus, Epstein–Barr virus, vesicular stomatitis virus, coronavirus, Kaposi's sarcoma-associated herpes virus and human immunodeficiency virus depend on Bcl-2-, Bcl-xL- and Bcl-w-mediated mitochondria-initiated apoptosis.[8–16] In addition to mitochondria-initiated apoptosis, the replication of these microbes is associated with the caspase-8-FADD (FAS-associating death domain-containing protein)-mediated apoptosis pathway.[17] We hypothesised that the chemical inhibitors of Bcl-2, Bcl-xL and Bcl-w could accelerate the death of virus-infected cells by enhancing caspase-mediated cross-talk between mitochondria and death receptor apoptosis pathways.

We show that anticancer ABT-263, ABT-737 and ABT-199 accelerate the death of non-cancerous mammalian cells infected with IAV and other viruses through the mutual amplification of the caspase-9-mediated mitochondria-initiated apoptosis by the IAV-initiated caspase-8-mediated apoptosis. Moreover, we show that the premature cell death limits the innate immune responses to viral infections and lowers the survival rates of infected animals. Our results suggest that ABT-263, ABT-737 and ABT-199 may be hazardous for cancer patients with viral infections.

Results

Anticancer agent ABT-263 accelerates death of virus-infected cells. Bcl-xL, Bcl-2 and Bcl-w are components of a cell-signalling network that governs cell survival and cell death in response to different stimuli such as viruses. We hypothesised that chemical inhibitors of Bcl-xL, Bcl-2 and Bcl-w could modulate the survival and death of virus-infected cells. We studied the effect of the anticancer agent ABT-263 on the survival of non-cancerous human macrophages in response to IAV infection.[18,19] Cells were treated with ABT-263, infected with IAV or mock, and cell survival was monitored at the indicated times. At non-cytotoxic concentrations, ABT-263 accelerated the death of IAV-infected cells (Figure 1a). The cell death was dependent on the dose of ABT-263 and on the multiplicity of the viral infection (Figures 1b and c). Interestingly, ABT-263 treatment only slightly attenuated the production of infectious virus particles (Figure 1d). Thus, at non-cytotoxic concentrations, anticancer ABT-263 sensitises non-cancerous cells to IAV-induced death.

Next we studied the effect of ABT-263 and its analogues on the death IAV-infected cells. We found that the structural analogues of ABT-263, ABT-737 and ABT-199 accelerated the death of IAV-infected human macrophages. By contrast, two other Bcl-xL-, Bcl-2- and Bcl-w-inhibitors – gossypol and TW-37 – were ineffective in the sensitisation of cells to IAV-induced death (Figure 2a; Supplementary Figure 1). The effect of ABT-263 was not restricted to a specific macrophage preparation, cell line or IAV strain (Figures 2b and c). Furthermore, ABT-263 accelerated the death of various cell types infected with influenza B (Orthomyxoviridae), Bunyamwera (Bunyaviridae), Semliki Forest and Sindbis (Togaviridae), Herpes Simplex 1 and 2 (Herpesviridae), Vaccinia (Poxiviridae), Measles (Paramyxoviridae), echovirus 6 (Picornaviridae), but not with Kaposi's sarcoma-associated herpes (Herpesviridae), Tick-borne encephalitis and dengue viruses (Flaviviridae) (Figure 2d and Supplementary Figure 2). These results suggest that ABT-263 and its structural analogues sensitise cells to virus-mediated killing and confirmed that Bcl-xL, Bcl-2 and Bcl-w are essential for cell survival upon viral infection.

Potential mechanism of action of ABT-263 in infected cells. To address the mechanism of action of ABT-263 in virus-infected cells, we first analysed the stage at which IAV infection ABT-263 triggers cell death using three known inhibitors of IAV infection: obatoclax, saliphenylhalamide and gemcitabine, which target myeloid cell leukaemia-1

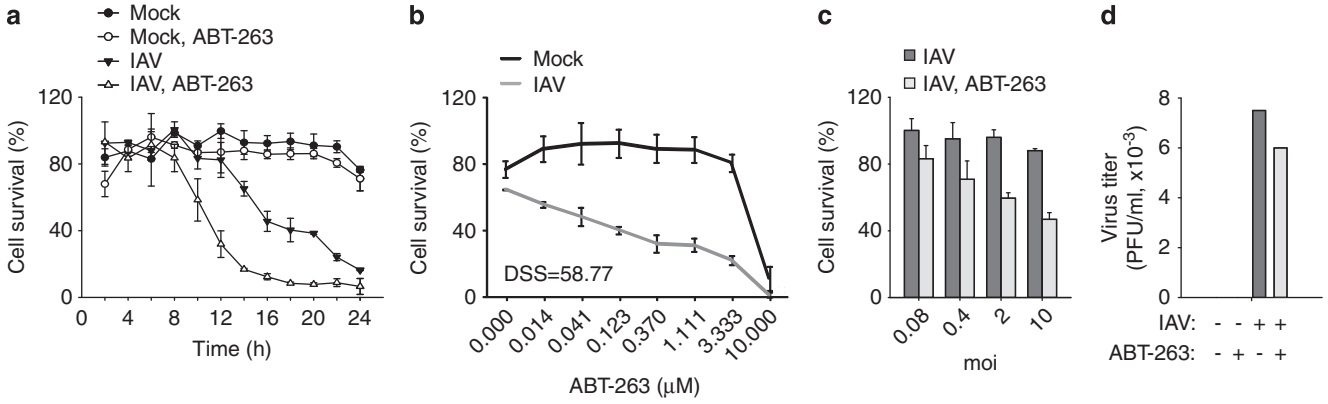

Figure 1 ABT-263 accelerates the death of primary human macrophages. (**a**) Human monocyte-derived macrophages were non- or ABT-263-treated (0.4 μM) and mock- or IAV-infected (WSN, moi 10), and cell viability was measured using a CTG assay at the indicated time points. (**b**) Macrophages were treated with increasing concentrations of ABT-263 and mock- or IAV-infected (WSN, moi 10), and cell viability was measured using a CTG assay 11 h after infection. The DSS was calculated. (**c**) Macrophages were non- or ABT-263-treated (0.4 μM) and infected with different moi of IAV (WSN), and cell viability was measured using a CTG assay 11 h after infection. (**d**) Macrophages were non- or ABT-263-treated (0.4 μM) and mock- or IAV-infected (WSN, moi 0.1), and virus production was determined 24 h after infection. All error bars, s.d. ($n=3$)

(Mcl-1), vacuolar ATPase (v-ATPase) and ribonucleotide reductase (RNR), respectively.[20,21] Mcl-1 and v-ATPase are necessary for endocytic uptake of IAV in cytoplasm, whereas RNR is essential for viral RNA transcription and replication in the nuclei of infected cells. We found that obatoclax and saliphenylhalamide, but not gemcitabine, rescued IAV-infected ABT-263-treated retinal pigment epithelium (RPE) cells from death (Figures 3a–c). Second, we performed a time-of-compound-addition experiment, which demonstrated that ABT-263 killed IAV-infected RPE cells independently of the time of its addition (Figure 3d). These results indicate that ABT-263 sensitises cells to death at multiple stages of IAV infection following virus endocytic uptake.

It was shown that ABT-263 targets Bcl-xL, Bcl-2 and Bcl-w in the mitochondria and disrupts their interactions with Bad, Bax and Bak proteins to initiate cancer cell death.[22] We tested whether ABT-263 affects these interactions in non-cancerous IAV-infected human cells. Our immunofluorescence experiment showed – and immuno-precipitation (IP) experiment confirmed – that at non-cytotoxic concentrations, ABT-263 displaced Bad from Bcl-xL and the mitochondria, and the IAV facilitated this process (Figure 4 and Figure 5). Thus, ABT-263 can destabilise the interaction of Bcl-xL, Bcl-2 and Bcl-w with Bad, Bax and Bak in the mitochondria of non-cancerous cells infected with IAV.

In cells, the Bcl-xL, Bcl-2 and Bcl-w interactions are not limited to Bad, Bax and Bak. Bcl-xL also interacts with voltage-dependent anion-selective channel protein 1 (VDAC),

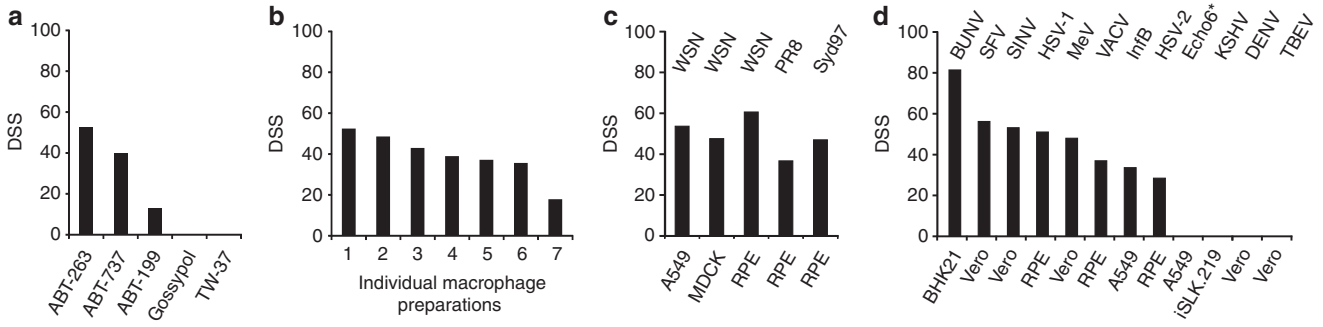

Figure 2 ABT-263 and its structural analogues accelerate the death of cell lines infected with IAV and several other viruses. (**a**) Human monocyte-derived macrophages were treated with ABT-263, ABT-737, ABT-199, gossypol or TW-37 and mock- or IAV-infected (WSN, moi 10), and DSS was estimated 11 h after infection. (**b**) Monocyte-derived macrophages from seven volunteers were treated with ABT-263 and mock- or IAV-infected (WSN, moi 10), and DSS was estimated 11 h after infection. (**c**) Different cell types were treated with ABT-263 and mock-infected or infected with different IAV strains (moi 10), and DSS was estimated 11 h after infection. (**d**) Different cell types were treated with ABT-263 and mock-infected or infected with different viruses as indicated (moi from 2 to 10), and DSS was estimated. Echo6* – —for more details see Supplementary Figure 2b

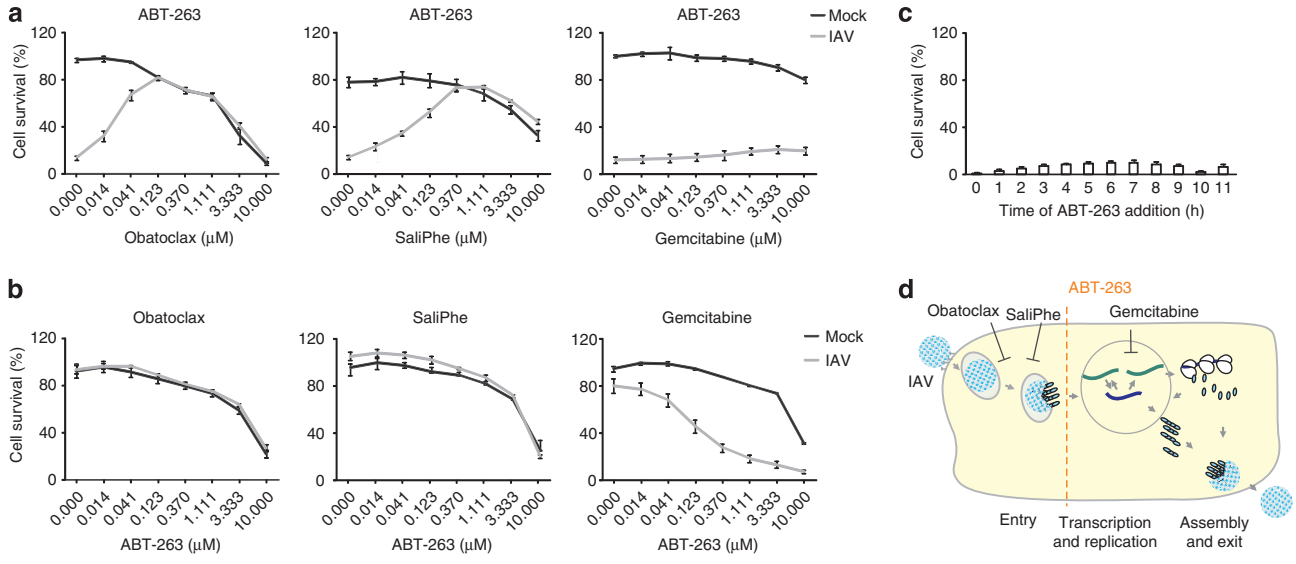

Figure 3 Obatoclax and SaliPhe but not gemcitabine inhibit the ABT-263-mediated death of IAV-infected RPE cells. (**a**) RPE cells were treated with ABT-263 (0.4 μM) and with increasing concentrations of obatoclax, SaliPhe or gemcitabine. Cells were mock- or IAV-infected (WSN, moi 10), and cell viability was measured using a CTG assay 24 h after infection. (**b**) RPE cells were treated with obatoclax (1 μM), SaliPhe (1 μM) or gemcitabine (10 μM) and with increasing concentrations of ABT-263. Cells were mock- or IAV-infected (WSN, moi 10), and cell viability was measured using a CTG assay 24 h after infection. (**c**) RPE cells were IAV-infected (WSN, moi 10) and treated with ABT-263 (0.4 μM) every hour. Cell viability was measured using a CTG assay 24 h after infection. (**d**) Schematic representation showing the stage of IAV replication cycle at which ABT-263 triggers cell death. All error bars, s.d. ($n=3$)

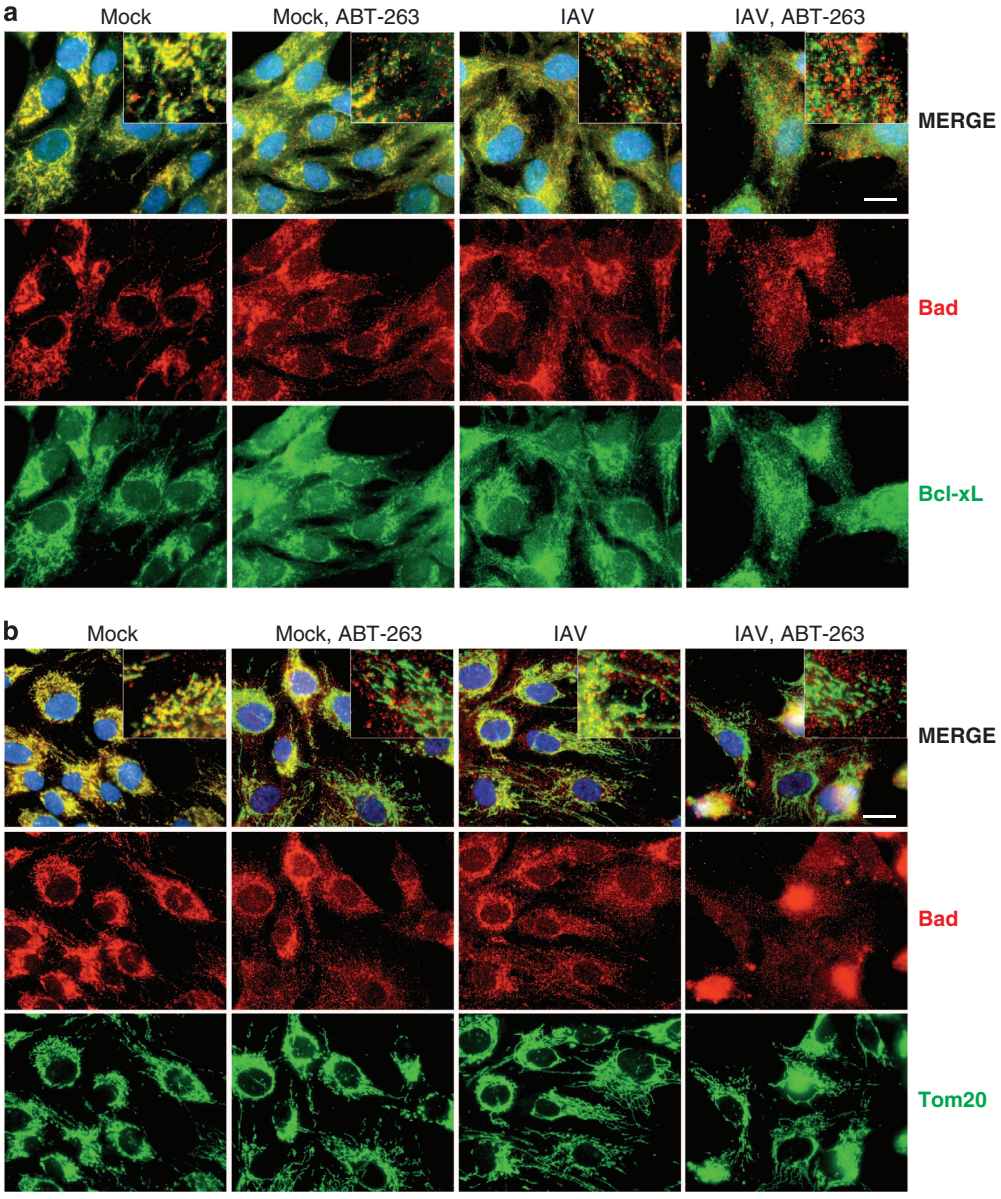

Figure 4 Simultaneous ABT-263 treatment and IAV infection of RPE cells displace Bad from Bcl-xL and mitochondria. (**a**) RPE cells were non- or ABT-263-treated (0.4 μM) and mock- or IAV-infected (WSN, moi 30), fixed 6 h after infection, and Bad and Bcl-xL were imaged by an immunofluorescence assay. (**b**) RPE cells were treated as in (**a**) and Bad and mitochondria (Tom20) were imaged using an immunofluorescence assay. Nuclei are stained by DAPI. Scale bars, 10 μm

Bcl-2-interacting mediator of cell death (Bim), DMN1L (dynamin-1-like protein), Becn1 (beclin-1), PGAM5 (phosphoglycerate mutase 1), PUMA (p53 upregulated modulator of apoptosis), p53, IKZF3 and HEBP2, whereas Bcl-2 also interacts with APAF1, BNIPL, MRPL41, TP53BP2, FKBP8, BAG1, RAF1, EGLN3 and G0S2.[23,24] However, the composition of Bcl-xL and Bcl-2 interactions could differ in different cell types. A combination of IP and mass spectrometry revealed that Bcl-xL interacts with Bad, Bax and Bak, as well as with UACA, PAWR, NUAK1, DAPK1, FLII, LRRFIP2, TOLLIP, TRIM21, H2B, DHX9, 14-3-3, various cytoskeleton proteins and viral HA (hemagglutinin), M1, NS1, NP (nucleoprotein) proteins in RPE cells (Supplementary Tables). Bcl-xL interactions with pattern recognition receptors (PPRs) such as LRRFIP2, H2B and DHX9 indicate that Bcl-xL is potentially involved in sensing viral nucleic acids, and Bcl-xL interactions with FLII, TOLLIP and LRRFIP2 indicate that it could be also involved in the Toll-like receptor 4 (TLR4) signalling cascade. Thus, we identify novel interacting partners for Bcl-xL, and possibly Bcl-2 and Bcl-w, which are specific but not limited to human non-cancerous RPE cells.

The disruption of Bcl-xL, Bcl-2 and Bcl-w interactions with newly identified partners by ABT-263 may contribute to IAV-mediated death of cells. We tested the effect of ABT-263 on interactions between Bcl-xL and its newly identified protein partners in IAV- and mock-infected RPE cells. An SDS-PAGE analysis of immuno-precipitated Bcl-xL-interacting proteins demonstrated the differences in the protein compositions of

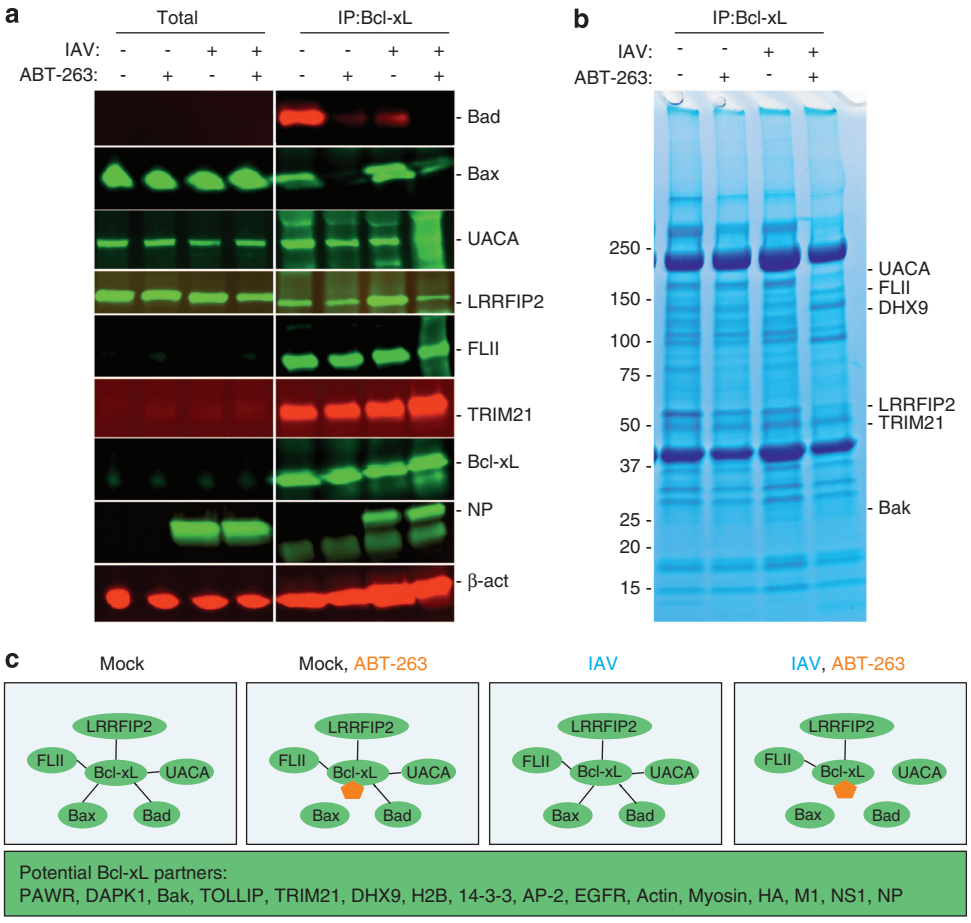

Figure 5 Simultaneous ABT-263 treatment and IAV infection of RPE cells displaces Bad, Bax and UACA from Bcl-xL. (**a**) RPE cells were non- or ABT-263-treated (0.4 μM) and mock- or IAV-infected (WSN, moi 10), and total cell lysates were obtained 6 h after infection. Bad, Bax, UACA, LRRFIP2, FLII, TRIM21, Bcl-xL, NP and β-actin (loading control) were analysed using western blotting in total lysates and immunoprecipitates by anti-Bcl-xL antibodies. (**b**) RPE cells were treated as in (**a**), lysates were immuno-precipitated by anti-Bcl-xL antibodies and analysed using Coomassie staining. (**c**) Schematic representation showing a mechanism of ABT-263 action during IAV infection 6 h after infection. ABT-263 is shown in orange

IPs (Figure 5b). Mass spectrometry, followed by an immonoblot analysis of protein candidates, showed that ABT-263, in combination with IAV, displaced UACA and Bax from Bcl-xL, in addition to Bad (Figures 5a and b). Thus, ABT-263 at non-cytotoxic concentrations alters the composition of Bcl-xL and perhaps of Bcl-2 and Bcl-w interactions in IAV-infected cells (Figure 5c).

Both ABT-263 and IAV activate caspase-8, -9, -3 and -7 to trigger cell death.[5,25] We monitored the activation of caspase-8, -9 and 3/7 in response to ABT-263 treatment and IAV infection in RPE cells over time. We observed that a combination of ABT-263 treatment and IAV infection resulted in the enhancement of caspase-8, -9, -3 and -7 activities, and this coincided with a decline of RPE cell viability (Figures 6a and b). In IAV-infected cells, activated caspases cleaved their substrates, such as Bid, and disrupted basic cellular pathways and functions, which resulted in an inhibition of the transcription and translation of cellular and viral mRNA and a reduction in the production of infectious IAV virions (Supplementary Figure 3). Thus, ABT-263 alters Bcl-xL, and perhaps Bcl-2 and Bcl-w interactions, and this activates caspase-8, -9, -3 and -7 to trigger the death of IAV-infected cells.

Interestingly, in RPE cells transfected with viral RNA (vRNA), ABT-263 was also able to stimulate caspase-9, -3 and -7 activity and, weakly, caspase-8 (Figure 6c). The caspase activation was dependent on the dose of ABT-263 and the concentration of transfected vRNA (data not shown). However, this was insufficient to trigger the death of vRNA-transfected RPE cells (Figure 6d). This indicates that ABT-263 can trigger cell death in response to replicating virus.

To test whether ABT-263-mediated premature death of infected cells alters the innate cellular immune responses, we analysed the production of cytokines in IAV-infected RPE cells in response to ABT-263 treatment (Figure 6e). Cytokine profiling revealed that ABT-263 treatment attenuated the IAV-mediated production of RANTES, interleukin (IL)-6, IL-8, IP-10, CCL2 (C–C motif chemokine 2), CXCL1, interferon (IFN)-β and IFN-λ, but stimulated the production of IL1ra (interleukin-1 receptor antagonist protein, IL-1F3). A similar result was obtained with ABT-737 and ABT-199 (Supplementary Figure 4). Interestingly, in vRNA-transfected RPE cells, ABT-263 was an ineffective inhibitor of RANTES, IL-6, IL-8, IFN-β and IFN-λ production because these cells remained alive. Thus, ABT-263 induces premature death of

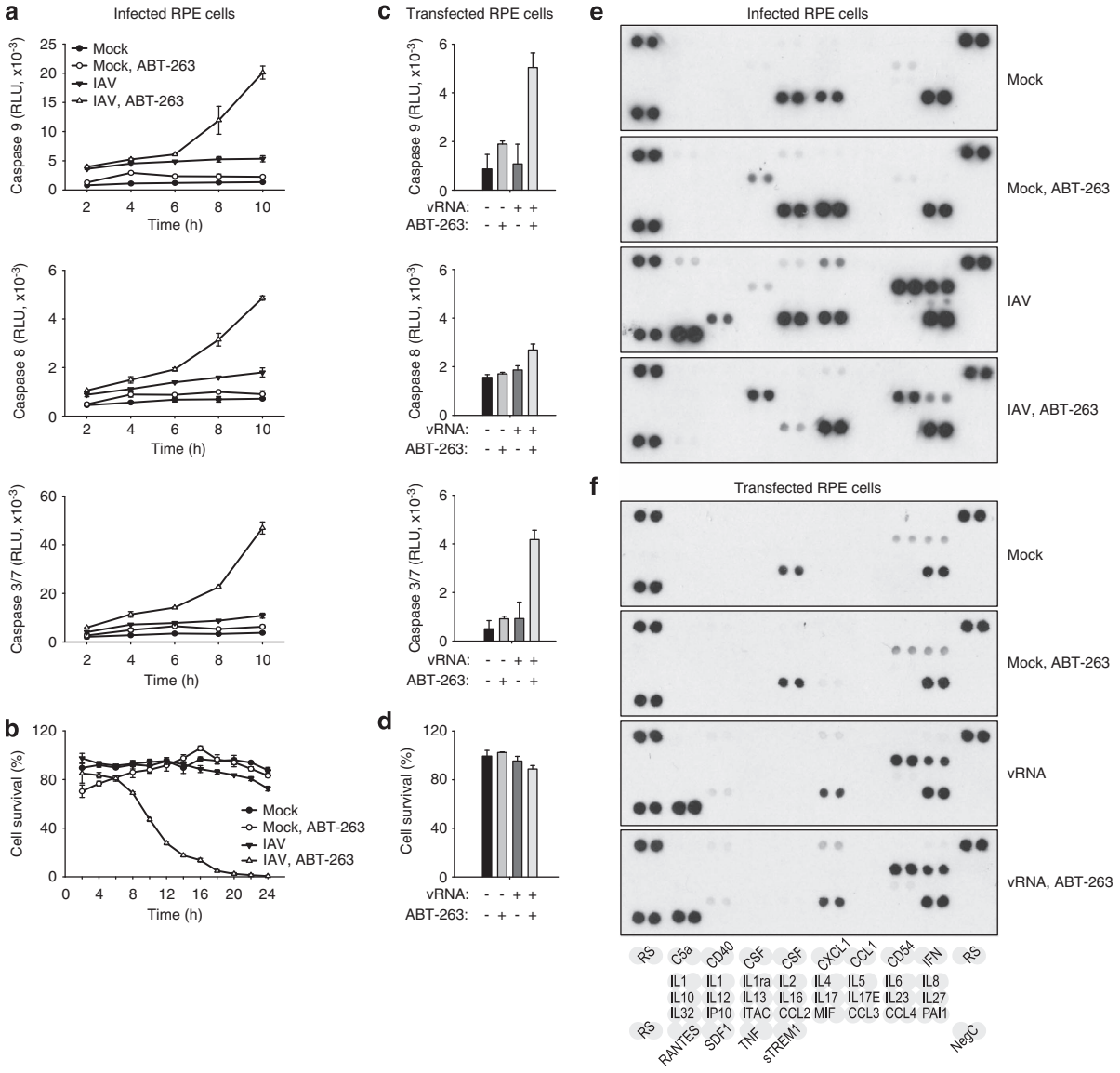
a
Infected RPE cells
Caspase 9 (RLU, x10-3)
Mock
Mock, ABT-263
IAV
IAV, ABT-263
Time (h)
Caspase 8 (RLU, x10-3)
Caspase 3/7 (RLU, x10-3)
b
Cell survival (%)
c
Transfected RPE cells
vRNA:
ABT-263:
d
e
Infected RPE cells
Mock
Mock, ABT-263
IAV
IAV, ABT-263
f
Transfected RPE cells
vRNA
vRNA, ABT-263
RS
C5a
CD40
CSF
CSF
CXCL1
CCL1
CD54
IFN
RS
IL1
IL1
IL1ra
IL2
IL4
IL5
IL6
IL8
IL10
IL12
IL13
IL16
IL17
IL17E
IL23
IL27
IL32
IP10
ITAC
CCL2
MIF
CCL3
CCL4
PAI1
RS
RANTES
SDF1
TNF
sTREM1
NegC

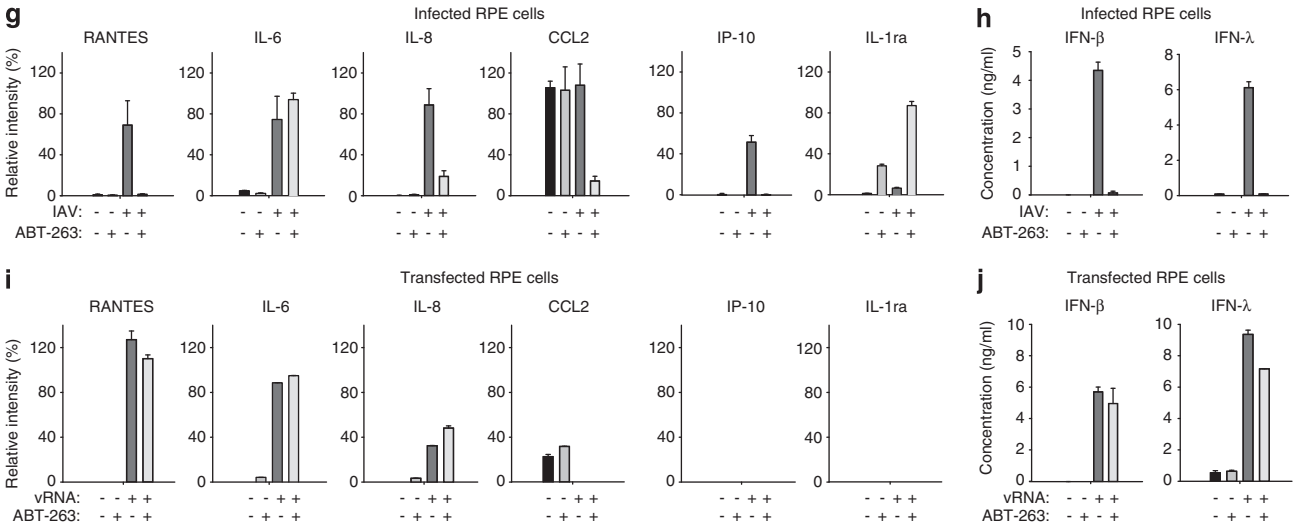
g
Infected RPE cells
RANTES
IL-6
IL-8
CCL2
IP-10
IL-1ra
Relative intensity (%)
IAV:
ABT-263:
h
IFN-β
IFN-λ
Concentration (ng/ml)
i
Transfected RPE cells
vRNA:
j

virus-infected cells and limits the production of cellular antiviral and pro-inflammatory responses.

ABT-263 lowers survival rates of IAV-infected mice by imbalancing the host's innate immune responses. We tested the effect of ABT-263 in a standard mouse model for influenza infection.[26] Mice were challenged with one lethal dose of mouse-adapted IAV, followed by a treatment with 50 mg/kg ABT-263 three times at 12-h intervals. The first dose of ABT-263 was given 48 h after infection. Kaplan–Meier survival curves showed that 100% of the ABT-263-treated IAV-infected animals died (or had to be euthanised due to excessive weight loss), whereas 60% of IAV-infected mock-treated animals recovered from the IAV infection (Figure 7a). The mouse survival rates were dependent on the dose of ABT-263 and the viral load (data not shown).

To further investigate the effect of ABT-263 treatment on IAV-infected mice, four mice in each of the different treatment groups were killed 6 days after infection, and the lungs were collected. These lungs were used for histology as well as for titration of the lung viral load, caspase activity and cytokine levels. The ABT 263 treatment was ineffective in viral replication (Figure 7b), caspase-3/7 activation (Figure 7c) or lung inflammation (Figure 7d), compared with untreated IAV-infected mice. We, however, observed a significant imbalance in cytokine production in ABT-263-treated IAV-infected mice in comparison with untreated IAV-infected mice (Figures 7e and f). This imbalance likely resulted in an inability of the immune system to clear the virus, eventually leading to death of the virus-infected ABT-263-treated animals.

Discussion

We here show that the anticancer ABT-263 and its structural analogues ABT-199 and ABT-737 accelerate the death of virus-infected cells and attenuate cellular antiviral and pro-inflammatory responses. Based on our results, we propose a mechanism of compound action in virus-infected non-cancerous cells (Figure 8). In our model, ABT-263, ABT-199 and ABT-737 bind Bcl-xL, Bcl-2 and Bcl-w and deactivate these cellular 'fuses' by altering their interactions with pro-apoptotic Bad, Bax and UACA in virus-infected cells. Bax and Bad dissociation from the 'fuses' mediate the release of apoptogenic molecules, including cytochrome *c*, from the mitochondria. Cytochrome *c* forms complexes with 'Bcl-xL-free' UACA, APAF1 and pro-caspase-9. Caspase-9 becomes activated in this complex, empowering it to activate caspase-3 and -7 which, in turn, activates caspase-8. Caspase-8 is also activated through a virus-induced FADD-mediated apoptosis pathway. Active caspase-8 cleaves Bid, and the cleaved Bid accelerates the mitochondrial caspase-9-mediated apoptosis pathway. Thus, the mutual amplification of caspase-8, -9, -3 and -7 results in a dramatic increase of the quantity and repertoire of proteolysed vital cell proteins, which potentiate the transition of the apoptotic process to the execution 'no return' phase of cell demise.

The premature cell death triggered by the inhibition of Bcl-xL, Bcl-2 and Bcl-w prevents the development of cellular antiviral and pro-inflammatory responses that are initiated by cellular PPRs such as RIG-I (retinoic acid inducible gene-I) and MDA5 in response to viral components.[27–29] Surprisingly, we found several PPRs (such as LRRFIP2, DHX9, H2B and components of TLR4-signalling pathway such as FLII, LRRFIP2 and TOLLIP) associated with Bcl-xL in mock- and IAV-infected human RPE cells. This indicates that Bcl-xL, Bcl-2 and Bcl-w regulate caspase-9-mediated apoptosis through PPRs-mediated recognition of virus components (such as vRNA).

We further observed an imbalance in cytokine production in ABT-263-treated IAV-infected mice, associated with an inability of the immune system to clear the virus, and eventually lowering the survival rates of infected animals. Note that mouse survival rates were dependent on the dose of ABT-263 and viral load. Our results, nevertheless, warrant against potential hazardous effects of therapeutic inhibition of Bcl-xL, Bcl-2 and Bcl-w when using ABT-263 and its derivatives in cancer patients with viral infections.

In conclusion, anticancer therapeutics may accelerate or attenuate microbial infection in cancer patients by targeting host functions essential for host–microbe interplay. However, anticancer programs have neglected the possibility of evaluating the effects of investigational small molecules on this interplay. Preclinical trials are typically performed on pathogen-free mice with xenotransplanted human tumour cells, and early stages of clinical trials focus on tumour regression and long-term survival without taking into account the potential impact of the chemotherapeutic agent in conjunction with underlying or overt viral infection of the patients. Our study sets an example for addressing the impact of anticancer molecules on the microbe–host interplay and the therapeutic outcome in a background of microbial infection.

Figure 6 Simultaneous ABT-263 treatment and IAV infection of RPE cells accelerates IAV-mediated apoptosis and dysregulates host cell cytokine production. (**a**) RPE cells were non- or ABT-263-treated (0.4 μM) and mock- or IAV-infected (WSN, moi 3), and caspase-3/7, -8 and -9 activity was measured at the indicated time points. (**b**) RPE cells were non- or ABT-263-treated (0.4 μM) and mock- or IAV-infected (WSN, moi 10), and cell viability was measured using a CTG assay at the indicated time points. (**c**) RPE cells were mock or viral RNA (180 ng) transfected and non- or ABT-263-treated (0.4 μM), and caspase-3/7, -8 and -9 activity was measured 24 h after transfection. (**d**) RPE cells were treated as in (**c**), and cell viability was measured using the CTG assay 24 h after transfection. All error bars, s.d. ($n=3$). (**e**) RPE cells were treated as in (**b**), cell culture supernatants were collected 24 h after infection, and cytokine levels were determined using a human cytokine array panel A kit. (**f**) RPE cells were treated as in (**c**), cell culture supernatants were collected 24 h after transfection, and cytokine levels were determined using a human cytokine array panel A kit. (**g**) RPE cells were treated as in (**b**), and levels of RANTES, IL-6, IL-8, CCL2, IP-10 and IL1ra were determined using a human cytokine array panel A kit ($n=2$) and (**h**) IFN-β and λ were determined by ELISA ($n=3$). (**i**) RPE cells were treated as in (**c**), and levels of RANTES, IL-6, IL-8, CCL2, IP-10 and IL1ra were determined using a human cytokine array panel A kit ($n=2$) and (**j**) IFN-β and λ were determined by ELISA ($n=3$)

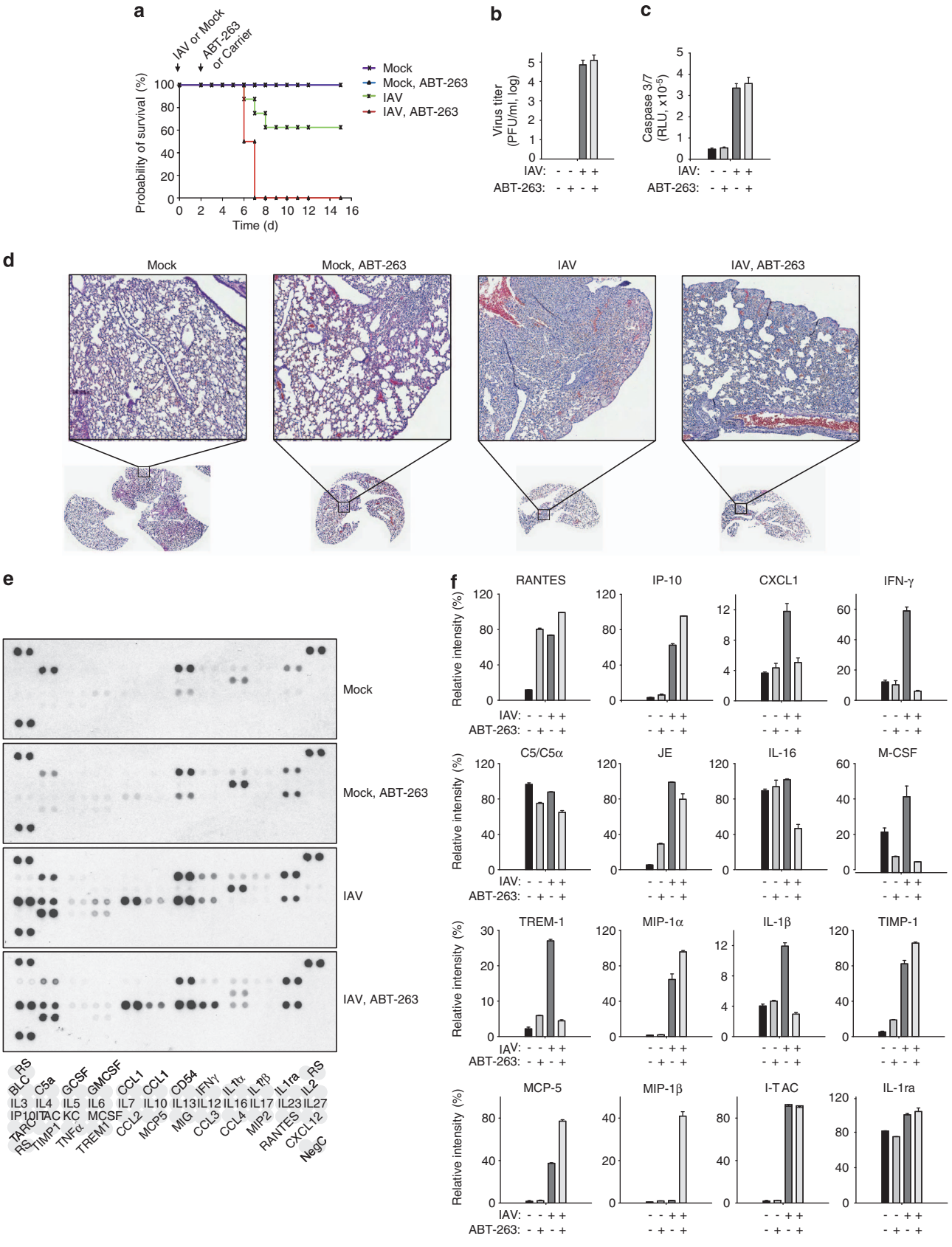
a
IAV or Mock
ABT-263 or Carrier
Probability of survival (%)
Time (d)
Mock
Mock, ABT-263
IAV
IAV, ABT-263
b
Virus titer (PFU/ml, log)
IAV:
ABT-263:
c
Caspase 3/7 (RLU, x10⁻⁵)
IAV:
ABT-263:
d
Mock
Mock, ABT-263
IAV
IAV, ABT-263
e
Mock
Mock, ABT-263
IAV
IAV, ABT-263
RS
BLC
C5a
GCSF
GMCSF
CCL1
CCL1
CD54
IFNγ
IL1α
IL1β
IL1ra
RS
IL3
IL4
IL5
IL6
IL7
IL10
IL13
IL12
IL16
IL17
IL23
IL27
IP10
ITAC
KC
MCSF
CCL2
MCP5
MIG
CCL3
CCL4
MIP2
RANTES
CXCL12
TARC
RS
TIMP1
TNFα
TREM1
NegC
f
RANTES
IP-10
CXCL1
IFN-γ
C5/C5α
JE
IL-16
M-CSF
TREM-1
MIP-1α
IL-1β
TIMP-1
MCP-5
MIP-1β
I-TAC
IL-1ra
Relative intensity (%)
IAV:
ABT-263:

Materials and Methods

Compounds, cells and viruses. ABT-263, ABT-737, gemcitabine, TW-37 and obatoclax were purchased from Selleck (Munich, Germany); ABT-199 were purchased from Active Biochem (Bonn, Germany); and gossypol was purchased from DTP/NCI. SaliPhe was provided by Jef De Brabander.[30] All the compounds were dissolved in 100% dimethyl sulfoxide (DMSO; Sigma-Aldrich, St. Louis, MO, USA) to 10 mM stock solutions and stored at −80 °C until use.

Human macrophages were differentiated from the peripheral blood mononuclear cells isolated from healthy individuals and from buffy coats of the voluntary blood donors from Finnish Red Cross as previously described.[31] Human telomerase reverse transcriptase-immortalized retinal pigment epithelial (hTERT-RPE), Madin–Darby canine kidney (MDCK), monkey Vero-E6, human adenocarcinomic alveolar basal epithelium (A549), doxycycline-inducible human endothelial SLK cell line latently infected with a recombinant KSHV.219 (Kaposi's sarcoma-associated herpes virus) virus (iSLK.219) and baby hamster kidney (BHK-21) cells were cultured as described.[31,32] All cells were grown at 37°C and 5% CO_2.

The infection of macrophages, RPE, MDCK, A549, BHK-21 and Vero-E6 cells with influenza A/WSN/33 (WSN; H1N1), A/PR/8/34 (PR8; H1N1), A/Sydney/5/1997 (Syd97; H3N2), B/Shandong/7/97 (InfB), human echovirus 6 (Echo6), sindbis (SINV), semliki forest (SFV), bunyamwera (BUNV), measles (MeV), herpes simplex 1 and 2 (HSV-1, HSV-2), tick born encephalitis (TBEV), dengue (DENV) and vaccinia (VACV) viruses was done as described previously.[31,32] KSHV production was induced in iSLK.219 cells with 0.2 μg/ml doxycycline and 1.35 μM sodium butyrate.[33] Titres of infectious viruses were determined as described.[26,31]

Compound efficacy testing *in vitro*. The compound efficacy testing was performed in 96-well plates in human macrophages, RPE, A549, MDCK, Vero-E6 and iSLK.219 cells. Typically, cells were seeded in 100 μl of an appropriate cell growth medium and grown for 24 h. The growth medium was changed to an appropriate virus inoculum[31] and the studied compounds were added into the medium; DMSO was added to the control wells. The cells were infected with viruses at a multiplicity of infection (moi) of 0.1–10 or non-infected (mock). Cell viability was measured using a Cell Titre Glo assay (CTG; Promega, Southampton, UK). Luminescence was read with PHERAstar FS plate reader (BMG Labtech, Ortenberg, Germany).

We used drug sensitivity scoring (DSS) to calculate the efficacy of ABT-263. Briefly, the dose–response curves were fitted based on a four-parameter logistic model using the GraphPad Prism 5 software (http://www.graphpad.com/scientific-software/prism/). Based on the estimated model parameters, quantitative responses were calculated and expressed as DSS values. DSS summarises the area under the dose–response curve over the entire dose range relative to the total area between 10% of the threshold and 100% of the inhibition. Further, to favour on-target responses over off-target responses, the integrated response was divided by the logarithm of the bottom asymptote of the logistic model. To assess the selective response of a compound to a virus-induced cell death, a differential DSS was calculated by subtracting the mock control DSS (no virus) from the viral DSS.

Compound efficacy testing *in vivo*. Specifically pathogen-free 6- to 7-week-old female BALB/c mice (Charles Rivers Laboratories, Lentilly, France) were used. The animals were housed in a temperature-controlled environment with 12-h light/dark cycles, and they received food and water *ad libitum*. Each group contained 14 mice. Mice were inoculated intranasally with 50 μl PBS with or without two LD50 of mouse-adapted A/PR/8/34 strain [26,34].[26] At 48 hpi, mice received the first oral dose of ABT-263, followed by two other doses at 12-h intervals. ABT-263 was dosed at 50 mg/kg in carrier (10% ethanol, 30% polyethylene glycol 400 and 60% Phosal 50 PG); an equal volume of carrier only was fed to the mock treatment group. This dosing of ABT-263 was based on previously reported toxicity study on mice.[22] Body weight was monitored daily and mice that had lost more than 30% of their initial body weight were euthanised by cervical dislocation. The survival data of the mouse experiments were analysed using SigmaStat 11.0 and the Gehan–Breslow Test. Statistical significance tests were performed with Student's *t*-test; $P<0.05$ was considered significant.

Four mice per treatment group were euthanised on day 6 post-infection, and lungs were collected. Lung homogenates were prepared from the right lobes in 1.5 ml of PBS using a microhomogeniser. The homogenate was cleared using centrifugation at 13 800 *g* for 15 min at 4 °C, and used for virus titre determination, cytokine profiling and caspase activation assays (described below). The left lobes of the lungs were fixed in neutral buffered 10% formalin, embedded in paraffin, cut with a microtome and 4 μm thick slices were stained with hematoxylin and eosin (H&E-staining). Slides were imaged using Panoramic 250 Flash slide scanner

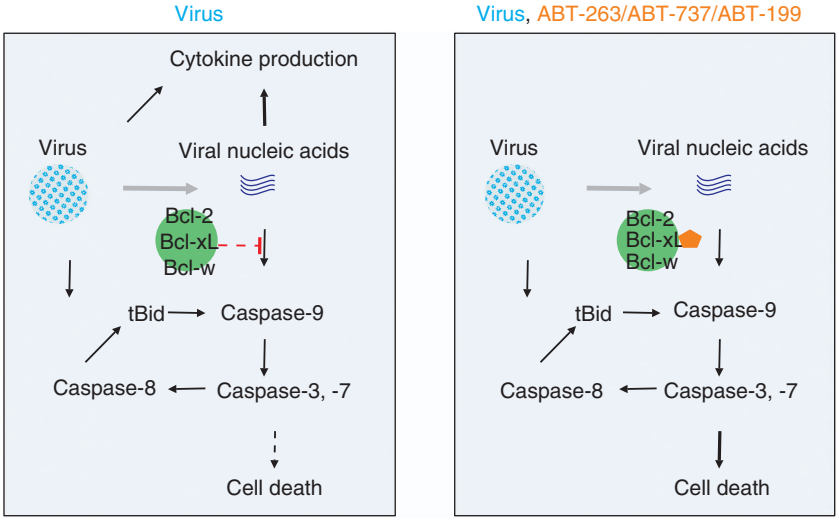

Figure 8 Potential mechanism of action of ABT-263 and its analogues in virus-infected cell

Figure 7 ABT-263 promotes the death of IAV-infected mice. (**a**) Kaplan–Meier survival curves of mice challenged with 50 μl PBS or two mouse LD50 doses of mouse-adapted PR8 influenza strain and treated with a carrier or ABT-263 (50 mg per kg body weight) in a carrier. ($n=10$ mice). (**b**) Viral titres from mouse lung homogenates at day 6 in each treatment group ($n=4$ mice). (**c**) Activity of caspase-3 and -7 in mouse lung homogenates at day 6 in each treatment group ($n=6$ mice). (**d**) Representative histochemical staining of lungs at day 6 in each treatment group. (**e** and **f**) Cytokine levels in mouse lung homogenates at day 6 in each treatment group were determined using a mouse cytokine array panel A kit ($n=2$). Error bars, s.d

(3DHistech, Hungary), and images were processed to virtual whole slides and uploaded to the web server as previously described.[35]

Biochemical assays. Cytokine profiling was performed using mouse lung homogenates or supernatants of compound-treated or non-treated, IAV-infected or non-infected cells. Cytokine levels were measured using mouse or human cytokine array panel A kits (R&D Systems, Minneapolis, MN, USA). Membranes were exposed to X-ray film, and films were scanned. Each image was analysed using the ImageJ software (http://rsbweb.nih.gov/ij/). In addition, the levels of TNF-α (tumour necrosis factor), IFN-β and λ in the cell supernatants were assayed with ELISA (PBL Interferon Source).

Caspases 8, 9 and 3/7 activity were measured with Caspase-Glo-8, -9 and -3/7 assays (Promega). Actin, NS1 and PB2 mRNA levels were assayed with reverse-transcription and strand-specific qPCRs as previously described.[36] Production of viral and cellular proteins was monitored using western blotting and autoradioautography. Briefly, RPE cells were washed twice with PBS and covered with 50 μl DMEM without methionine (Sigma-Aldrich) containing 10% BSA and S^{35} methionine (Perkin Elmer, Espoo, Finland), and incubated for 1 h at 37 °C. RPE cells were washed twice with PBS, lysed in 2 × SDS-loading buffer and sonicated. Lysates were loaded and proteins were separated on a gradient 4–20% SDS-polyacrylamide gel (SDS-PAGE; Bio-Rad, Helsinki, Finland). S^{35}-labelled proteins were monitored using radioautography and visualised using a Typhoon 9400 scanner (GE Healthcare, Helsinki, Finland).

For a genomic viral RNA (vRNA) transfection experiment, A/WSN/33 virus was grown in MDCK cells. Supernatants were collected at 24 hpi, and the virus was pelleted using ultracentrifugation at 285 000 g for 4 h. Viral RNA was purified using the RNA extraction kit (Qiagen, Hilden, Germany). The RNA was transfected into RPE cells using Lipofectamine 2000 (Life Technologies, Carlsbad, CA, USA) according to the manufacturer's instructions. Six hours after transfection, the Opti-MEM media were replaced with growth media with or without 0.4 μM ABT-263. After 18 h, the cell viability or caspase activity was measured.

Bcl-xL-associated factors were immuno-precipitated from infected and non-infected, ABT-263-treated or non-treated RPE cells using rabbit anti-Bcl-xL (1 : 200; cell signalling technology, Danvers, MA, USA) antibody as previously described.[37] Immuno-precipitated proteins were separated with SDS-PAGE and visualised by Coomassie staining. The entire lanes of SDS-PAGE were cut and the proteins were in-gel digested with trypsin. Resulting peptides were analysed using liquid chromatography–tandem mass spectrometry as previously described.[38] The mass spectrometry data were searched using in-house Mascot and the ProteinPilot interface against the SwissProt database. All of the reported protein identifications were statistically significant ($P < 0.05$).

For immunoblotting, proteins were separated using SDS-PAGE and transferred to a Hybond-LFP PVDF membrane. The membrane was blocked using 5% milk in Tris-buffered saline (TBS) and incubated with a primary guinea pig anti-NS1 (1 : 2000), rabbit anti-Bcl-xL (1 : 1000; cell signalling technology), rabbit anti-Bid (1 : 1000; cell signalling technology), rabbit anti-Bax (1 : 100; Santa Cruz Biotechnology, Heidelberg, Germany), mouse anti-Bad (1 : 200; Santa Cruz Biotechnology), rabbit anti-UACA (1 : 250; Sigma-Aldrich), rabbit anti-NP (1 : 500) or mouse anti-β-actin (1 : 2000; Thermo Fisher Scientific, Dreieich, Germany) antibody overnight at 4 °C. The membrane was washed three times for 10 min with TBS buffer containing 0.03% Tween 20 (Tween/TBS), and incubated for 4 h at 4 °C with the respective secondary antibodies conjugated to infrared dyes 680LT or 800CW (1 : 20,000, Li-Cor Biosciences, Koge, Denmark). After three washes for 10 min with Tween/TBS buffer and one with TBS, membranes were scanned using an Odyssey scanner (Li-Cor Biosciences).

For immunofluorescence experiments ABT-263 (0.4 μM) treated or non-treated RPE cells were infected with A/WSN/33 at moi 30. At 6 hpi, cells were fixed with 4% paraformaldehyde (in PBS). PBS with 1% BSA and 0.1% Triton X-100 was used for blocking and permeabilisation of the fixed cells and for dilution of antibodies. For detection of proteins, rabbit anti-Bcl-xL (1 : 200; clone 54H6; Cell Signalling Technology), mouse anti-BAD (1 : 100; clone c-7; Santa Cruz Biotechnology), rabbit anti-Tom20 (1 : 300; clone FL-145; Santa Cruz Biotechnology) antibodies were used. Secondary antibodies were anti-mouse Alexa Fluor 594 or anti-rabbit Alexa Fluor 488 conjugated antibodies (1 : 2000 or 1 : 1000; Life Technologies). Nuclei were counter-stained with DAPI. Images were captured using Nikon 90i microscope and processed using the NIS Elements AR software (Nicon Instruments, Melville, NY, USA).

Ethical issues. Viral infections were carried out under BSL-2 conditions and in compliance with regulations of the University of Helsinki (permit No 21/M/09). Buffy coat fractions of voluntary blood donors were obtained under permission from the Finnish Red Cross Blood Transfusion Service and approved by the ethical review committee of the University of Helsinki Central Hospital, Finland (165/13/03/00/2011). Collection of blood samples from volunteers was approved by the ethical review committee of the University of Helsinki Central Hospital, Finland (244/13/03/01/2012). Mouse influenza virus infection experiments were carried out under BSL-2+ conditions and were authorised by the Institutional Ethics Committee on Experimental Animals of the VIB Department for Molecular Biomedical Research at Ghent University.

Conflict of Interest

The authors declare no conflict of interest.

Acknowledgements. We thank Jenni Säilä and Sami Blom for technical assistance; Markus Vähä-Koskela, Richard M. Elliott, Jef K. De Brabander, Juha Klefström, Hannimari Kallio-Kokko, Anu Kantele, Johannes Kettunen, Antti-Pekka Sarin and Johanna Lampe for viruses, reagents and scientific assistance. We are grateful to all the voluntary blood donors. This work was supported by the Jane and Aatos Erkko Foundation, Centre for International Mobility (CIMO), the Academy of Finland Grants 255780, 138644 and 255852, and Robert A. Welch Foundation Grant I-1422.

1. Souers AJ, Leverson JD, Boghaert ER, Ackler SL, Catron ND, Chen J *et al.* ABT-199, a potent and selective BCL-2 inhibitor, achieves antitumor activity while sparing platelets. *Nat Med* 2013; **19**: 202–208.
2. Vandenberg CJ, Cory S. ABT-199, a new Bcl-2-specific BH3 mimetic, has *in vivo* efficacy against aggressive Myc-driven mouse lymphomas without provoking thrombocytopenia. *Blood* 2013; **121**: 2285–2288.
3. Davids MS, Letai A. ABT-199: taking dead aim at BCL-2. *Cancer cell* 2013; **23**: 139–141.
4. Cullen SP, Martin SJ. Caspase activation pathways: some recent progress. *Cell Death Differ* 2009; **16**: 935–938.
5. Mutlu A, Gyulkhandanyan AV, Freedman J, Leytin V. Activation of caspases-9, -3 and -8 in human platelets triggered by BH3-only mimetic ABT-737 and calcium ionophore A23187: caspase-8 is activated via bypass of the death receptors. *Br J Haematol* 2012; **159**: 565–571.
6. Xiao F, Gao W, Wang X, Chen T. Amplification activation loop between caspase-8 and -9 dominates artemisinin-induced apoptosis of ASTC-a-1 cells. *Apoptosis* 2012; **17**: 600–611.
7. Kantari C, Walczak H. Caspase-8 and bid: caught in the act between death receptors and mitochondria. *Biochim Biophys Acta* 2011; **1813**: 558–563.
8. Geng X, Huang C, Qin Y, McCombs JE, Yuan Q, Harry BL *et al.* Hepatitis B virus X protein targets Bcl-2 proteins to increase intracellular calcium, required for virus replication and cell death induction. *Proc Natil Acad Sci US A* 2012; **109**: 18471–18476.
9. Kraemer BF, Campbell RA, Schwertz H, Franks ZG, Vieira de Abreu A, Grundler K *et al.* Bacteria differentially induce degradation of Bcl-xL, a survival protein, by human platelets. *Blood* 2012; **120**: 5014–5020.
10. Ghigna MR, Reineke T, Rince P, Schuffler P, El Mchichi B, Fabre M *et al.* Epstein-Barr virus infection and altered control of apoptotic pathways in posttransplant lymphoproliferative disorders. *Pathobiology* 2013; **80**: 53–59.
11. Park J, Kang W, Ryu SW, Kim WI, Chang DY, Lee DH *et al.* Hepatitis C virus infection enhances TNFalpha-induced cell death via suppression of NF-kappaB. *Hepatology* 2012; **56**: 831–840.
12. Busca A, Saxena M, Kumar A. Critical role for antiapoptotic Bcl-xL and Mcl-1 in human macrophage survival and cellular IAP1/2 (cIAP1/2) in resistance to HIV-Vpr-induced apoptosis. *J Biol Chem* 2012; **287**: 15118–15133.
13. Pearce AF, Lyles DS. Vesicular stomatitis virus induces apoptosis primarily through Bak rather than Bax by inactivating Mcl-1 and Bcl-XL. *J Virol* 2009; **83**: 9102–9112.
14. Tan YX, Tan TH, Lee MJ, Tham PY, Gunalan V, Druce J *et al.* Induction of apoptosis by the severe acute respiratory syndrome coronavirus 7a protein is dependent on its interaction with the Bcl-XL protein. *J Virol* 2007; **81**: 6346–6355.
15. Cheng EH, Nicholas J, Bellows DS, Hayward GS, Guo HG, Reitz MS *et al.* A Bcl-2 homolog encoded by Kaposi sarcoma-associated virus, human herpesvirus 8, inhibits apoptosis but does not heterodimerize with Bax or Bak. *Proc Natl Acad Sci USA* 1997; **94**: 690–694.
16. Nencioni L, De Chiara G, Sgarbanti R, Amatore D, Aquilano K, Marcocci ME *et al.* Bcl-2 expression and p38MAPK activity in cells infected with influenza A virus: impact on virally induced apoptosis and viral replication. *Journal Biol Chem* 2009; **284**: 16004–16015.
17. Kepp O, Senovilla L, Galluzzi L, Panaretakis T, Tesniere A, Schlemmer F *et al.* Viral subversion of immunogenic cell death. *Cell Cycle* 2009; **8**: 860–869.
18. Davids MS, Letai A. Targeting the B-cell lymphoma/leukemia 2 family in cancer. *J Clin Oncol* 2012; **30**: 3127–3135.
19. Herold S, Ludwig S, Pleschka S, Wolff T. Apoptosis signaling in influenza virus propagation, innate host defense, and lung injury. *J Leukocyte Biol* 2012; **92**: 75–82.

20. Denisova OV, Kakkola L, Feng L, Stenman J, Nagaraj A, Lampe J *et al.* Obatoclax, saliphenylhalamide and gemcitabine inhibit influenza A virus infection. *J Biol Chem* 2012; **287**: 35324–35332.
21. Muller KH, Kakkola L, Nagaraj AS, Cheltsov AV, Anastasina M, Kainov DE. Emerging cellular targets for influenza antiviral agents. *Trends Pharmacol Sci* 2012; **33**: 89–99.
22. Tse C, Shoemaker AR, Adickes J, Anderson MG, Chen J, Jin S *et al.* ABT-263: a potent and orally bioavailable Bcl-2 family inhibitor. *Cancer Res* 2008; **68**: 3421–3428.
23. Follis AV, Chipuk JE, Fisher JC, Yun MK, Grace CR, Nourse A *et al.* PUMA binding induces partial unfolding within BCL-xL to disrupt p53 binding and promote apoptosis. *Nat Chem Biol* 2013; **9**: 163–168.
24. Renault TT, Chipuk JE. Getting away with murder: how does the BCL-2 family of proteins kill with immunity? *Ann N Y Acad Sci* 2013; **1285**: 59–79.
25. Xing Z, Harper R, Anunciacion J, Yang Z, Gao W, Qu B *et al.* Host immune and apoptotic responses to avian influenza virus H9N2 in human tracheobronchial epithelial cells. *Am J Respir Cell Mole Biol* 2011; **44**: 24–33.
26. Muller KH, Kainov DE, El Bakkouri K, Saelens X, De Brabander JK, Kittel C *et al.* The proton translocation domain of cellular vacuolar ATPase provides a target for the treatment of influenza A virus infections. *Br J Pharmacol* 2011; **164**: 344–357.
27. Wies E, Wang MK, Maharaj NP, Chen K, Zhou S, Finberg RW *et al.* Dephosphorylation of the RNA sensors RIG-I and MDA5 by the phosphatase PP1 is essential for innate immune signaling. *Immunity* 2013; **38**: 437–449.
28. Pothlichet J, Meunier I, Davis BK, Ting JP, Skamene E, von Messling V *et al.* Type I IFN triggers RIG-I/TLR3/NLRP3-dependent inflammasome activation in influenza A virus infected cells. *PLoS Pathogens* 2013; **9**: e1003256.
29. Le Goffic R, Pothlichet J, Vitour D, Fujita T, Meurs E, Chignard M *et al.* Cutting edge: influenza A virus activates TLR3-dependent inflammatory and RIG-I-dependent antiviral responses in human lung epithelial cells. *J Immunol* 2007; **178**: 3368–3372.
30. Lebreton S, Jaunbergs J, Roth MG, Ferguson DA, De Brabander JK. Evaluating the potential of vacuolar ATPase inhibitors as anticancer agents and multigram synthesis of the potent salicylihalamide analog saliphenylhalamide. *Bioorg Med Chem Lett* 2008; **18**: 5879–5883.
31. Denisova OV, Kakkola L, Feng L, Stenman J, Nagaraj A, Lampe J *et al.* Obatoclax, saliphenylhalamide, and gemcitabine inhibit influenza a virus infection. *J Biol Chem* 2012; **287**: 35324–35332.
32. Myoung J, Ganem D. Generation of a doxycycline-inducible KSHV producer cell line of endothelial origin: maintenance of tight latency with efficient reactivation upon induction. *J Virol Methods* 2011; **174**: 12–21.
33. Myoung J, Ganem D. Infection of lymphoblastoid cell lines by Kaposi's sarcoma-associated herpesvirus: critical role of cell-associated virus. *J Virol* 2011; **85**: 9767–9777.
34. El Bakkouri K, Descamps F, De Filette M, Smet A, Festjens E, Birkett A *et al.* Universal vaccine based on ectodomain of matrix protein 2 of influenza A: Fc receptors and alveolar macrophages mediate protection. *J Immunol* 2011; **186**: 1022–1031.
35. Lundin M, Lundin J, Helin H, Isola J. A digital atlas of breast histopathology: an application of web based virtual microscopy. *J Clin Pathol* 2004; **57**: 1288–1291.
36. Feng L, Lintula S, Ho TH, Anastasina M, Paju A, Haglund C *et al.* Technique for strand-specific gene-expression analysis and monitoring of primer-independent cDNA synthesis in reverse transcription. *BioTechniques* 2012; **52**: 263–270.
37. He C, Bassik MC, Moresi V, Sun K, Wei Y, Zou Z *et al.* Exercise-induced BCL2-regulated autophagy is required for muscle glucose homeostasis. *Nature* 2012; **481**: 511–515.
38. Ohman T, Lietzen N, Valimaki E, Melchjorsen J, Matikainen S, Nyman TA. Cytosolic RNA recognition pathway activates 14-3-3 protein mediated signaling and caspase-dependent disruption of cytokeratin network in human keratinocytes. *J Proteome Res* 2010; **9**: 1549–1564.

Supplementary Information accompanies this paper on Cell Death and Disease website (http://www.nature.com/cddis)